# OFDM Time and Frequency Synchronization by Spread Spectrum Pilot Technique

Tufvesson, Fredrik; Faulkner, Michael; Hoeher, Peter; Edfors, Ove

*Published in:*
Proc. 8th IEEE Communication Theory Mini Conference in conjunction to ICC'99, Vancouver, Canada, June 7-10, 1999

*DOI:*
10.1109/CTMC.1999.790248

1999

# OFDM Time and Frequency Synchronization by Spread Spectrum Pilot Technique

Fredrik Tufvesson[1], Mike Faulkner[2], Peter Hoeher[3] and Ove Edfors[1]

[1]Department of Applied Electronics, Lund University, Box 118, SE-221 00 Lund, Sweden, e-mail: Fredrik Tufvesson@tde.lth.se
[2]School of Communications and Informatics, Victoria University of Technology, Melbourne, Australia
[3]Information and Coding Theory Lab, University of Kiel, Kiel, Germany

*Abstract* – **Correct time and frequency synchronization is important for the performance of orthogonal frequency division multiplex (OFDM) systems. We evaluate a system where a pseudo noise sequence (PN-sequence) is used for estimation of these synchronization parameters. The PN-sequence is superimposed on the OFDM signal. The system is evaluated by means of the variance of the frequency estimation error and the probability for correct timing synchronization. Both theoretical and simulated results are presented. The proposed technique is very flexible and works also at low signal to noise ratios. The frequency offset range has been significantly increased compared to conventional OFDM synchronizer schemes.**

## I. Introduction

Time and frequency synchronization are two important issues for the performance of orthogonal frequency division multiplex (OFDM) systems. Correct frequency synchronization is crucial in order to preserve orthogonality of the sub-channels. Timing synchronization is necessary in order to locate the cyclic prefix and identify the start of new packets or frames. Often the synchronization process is divided into two parts, acquisition and tracking. Burst transmission acquisition includes a continuous search for new packets, finding the beginning of the symbols as well as the packets and making a coarse frequency estimate so that demodulation can be performed. For continuous transmission, acquisition means finding the start of symbols and frames and making a coarse frequency estimate. In tracking mode the synchronization parameters are continuously updated to keep the performance of the demodulator as good as possible under changing conditions.

Existing algorithms are often based on correlation of either a repeated [1][2][3] or a known [4][5] symbol. A correlation peak is achieved when the timing is correct and then the frequency offset estimate is achieved by the phase shift between certain samples. The distance between these samples determines the frequency offset range. When, e.g., the cyclic prefix is used as a repeated symbol the frequency offset range is limited to half the sub-channel spacing.

This paper presents a new method for acquisition and tracking of OFDM synchronization parameters, which is based on a continuous transmission of a pseudo noise (PN) sequence. Similar techniques has previously been proposed for synchronization of single carrier systems [6] and for frame synchronization in OFDM systems [7]. In this paper we propose and investigate a system for frequency and timing synchronization, including both symbol and frame synchronization. The system can cope with very large offsets, up to half the OFDM bandwidth, and gives the frequency estimate in one step. The synchronization signal has a sharp peak and is independent of the OFDM parameters used. It can be used for any length of the cyclic prefix and does not increase the transmitted bandwidth.

F.T. thanks The Royal Swedish Academy of Sciences for providing financial support and Dr. Shousheng He for motivating this work.

## II. Spread Spectrum Pilot Technique

The estimation of synchronization parameters is based on transmission of a PN-sequence which is *superimposed* on the OFDM information signal. The chip time of the PN-sequence is equal to or double the sample time in the OFDM system, depending on spectrum and sampling requirements. The sequences are synchronous and transmitted in the same band. Fig. 1 shows a block description of how the transmitted signal is generated. During acquisition the PN-sequence is sent without transmission of the information signal. After one or more PN-symbols, when the correct timing and carrier frequency have been found, the transmission of the information signal starts and the receiver enters the tracking mode, see Fig. 2. In tracking mode the amplitude of the PN-sequence can be chosen so that the distortion of the information symbol is small. The amplitude of the PN-sequence can be adjusted to a specific application and the synchronization scheme works for low signal to noise ratios. It is desirable to use a code length equal to or a multiple of the OFDM symbol length (including the cyclic prefix) so that correlation peaks occur at the symbol boundaries. For frame synchronization it is sometimes advantageous to use a long code.

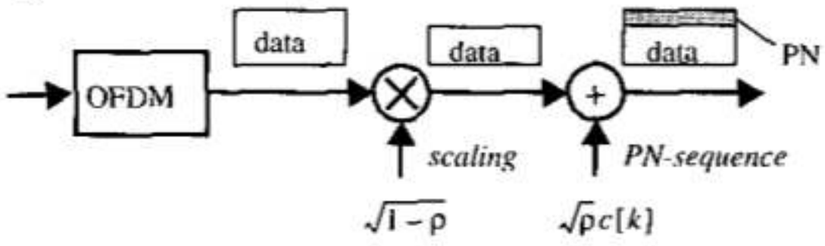


Fig. 1. Generation of the transmitted signal

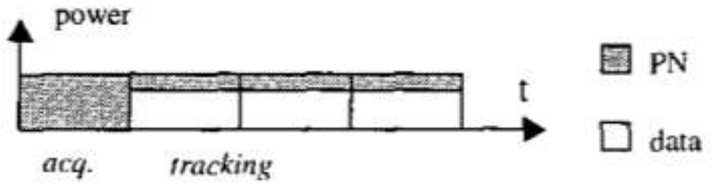


Fig. 2. Structure of the transmitted signal.

## III. System Description

In the analysis we assume an OFDM system with $M$ sub-channels, having a symbol time $T_s$ in an AWGN channel. The discrete time representation of the received base band signal is

$$r[k] = s[k] + n'[k] \tag{1}$$
$$= (\sqrt{\rho}\sigma_s c[k] + \sqrt{1-\rho}\sigma_s d[k]) e^{j\left(\frac{2\pi\varepsilon_c k}{M} + \theta_c\right)} + n'[k].$$

where $c[k]$ is the transmitted PN-sequence, $d[k]$ is the OFDM data sequence and $n'[k]$ is white Gaussian noise with spectral density $N_0$. Further, $\theta_c$ is the carrier phase and $\varepsilon_c = \Delta f \cdot T_s$ denotes the frequency offset to be estimated when normalized by the sub-channel spacing. Both the PN-sequence and the data sequence has unity power and the amount of power used for the PN-sequence is controlled by the code power ratio $\rho$. The received power is given by $\sigma_s^2 \equiv E_s/T_s = E[|s[k]|^2]$, whereas the noise power is given by $\sigma_n^2 \equiv (N_0/T_s) = E[|n[k]|^2]$. The received signal is despread by the local PN-sequence to get

$$c^*[k-a]r[k] = \sqrt{\rho}\sigma_s c^*[k-a]c[k]e^{j(2\pi\varepsilon_c k/M + \theta_c)} \tag{2}$$
$$+ \sqrt{1-\rho}\sigma_s d[k]c^*[k-a]e^{j(2\pi\varepsilon_c k/M + \theta_c)} + n[k].$$

For time synchronization we want to find the integer slip, $a$, between the two codes. For the purpose of time and frequency estimation, the two latter terms in (2) are acting as disturbances. For data demodulation, no code multiplication is performed in the receiver and the first and the last terms cause disturbances. The resulting SNR becomes $\rho\sigma_s^2/((1-\rho)\sigma_s^2 + \sigma_n^2)$ for the code sequence and $(1-\rho)\sigma_s^2/(\rho\sigma_s^2 + \sigma_n^2)$ for the data sequence. In acquisition mode, only the code sequence is sent and the code power ratio $\rho$ equals one. In tracking mode a low code power ratio is then used in order to minimize the impact on data transmission.

The despread signals are summed in groups of $K$ samples to get a so called sub-correlation. The synchronization signal, $\gamma[k, a]$, for a given slip, $a$, is then achieved as the sum of $L$ products between sub-correlations spaced $KP$ samples apart ($P$ is the delay in number of correlator lengths),

$$\gamma[k, a] = \sum_{l=0}^{L-1}\left[\left(\sum_{n=0}^{K-1} c^*[k-n-lK-a]r[k-n-lK]\right)\right. \tag{3}$$
$$\left.\left(\sum_{n=0}^{K-1} c^*[k-n-(l+P)K-a]r[k-n-(l+P)K]\right)^*\right].$$

Time synchronization is given by the absolute value of this signal whereas the frequency offset estimate is given by the phase. The synchronizer structure is given in Fig. 3. This scheme can be seen as a modification of the schemes in [4] and [5]. Here, the length of the sub-correlators is $K$ instead of 1 as in [5], and the differential detectors work on the sub-correlator outputs instead of the correlator outputs as in [4].

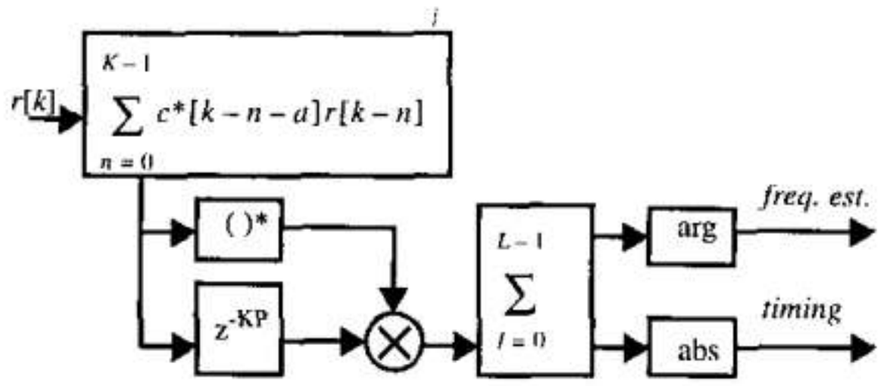

Fig. 3. Block diagram of the estimator.

## IV. Timing Estimator Performance

In this section we analyze the distribution of the timing metric in an AWGN channel. Firstly we analyze the case when the timing is correct and later when it is wrong. The calculations are quite tedious and therefore we just summarize the results and verify them by means of simulations. Often it is desirable to have a signal which is independent of received power. By normalizing $\gamma$ as $\lambda[k, a] = \gamma[k, a]/(LK^2\rho\sigma_s^2)$ we get a timing metric with a mean close to one when the timing is correct and just above zero when it is wrong.

### A. Correct Timing

When the timing is correct, $a$=0, the distribution of the timing metric can be analyzed in a similar way as in [3]. The frequency offset entails that the chips are not added totally in phase in the sub-correlator, which leads to an energy reduction. We assume that no ISI is present and $|\varepsilon_c| \ll M$. Normalizing the sub-correlator signal by $\sqrt{LK^2\rho\sigma_s^2}$ gives the normalized output, $\eta[k, 0]$, where [4]

$$\eta[k, 0] = \frac{1}{L}\mathrm{sinc}(\varepsilon_c K/M)\exp\left(j\frac{2\pi\varepsilon_c}{M}\left(k + \frac{1}{2}\right)\right) + n_\eta[k, 0]. \tag{4}$$

All differential products then add coherently since they have nearly the same phase. For medium and high SNR:s, the contribution from the noise vector perpendicular to the signal vector can be neglected. If we consider the data signal as Gaussian, or if $K$ is large, $|\lambda[k, 0]|$ can be approximated as a Gaussian variable with mean

$$E[|\lambda[k, 0]|] = \mathrm{sinc}^2(\varepsilon_c K/M) \tag{5}$$

and variance

$$var[\lambda[k, 0]] = \frac{((1-\rho)\sigma_s^2 + \sigma_n^2)\mathrm{sinc}^2(\varepsilon_c K/M)}{LK\rho\sigma_s^2}. \tag{6}$$

As seen in (6) the variance is inversely proportional to $LK$. The particular choice of correlator length has small impact on this product if the observation interval is kept constant. The

probability of missing the sync signal is therefore mainly determined by the observation interval and the equivalent SNR for the PN-sequence.

### *B. Incorrect Timing*

When the timing is wrong, $a \neq 0$, the sub-correlators do not peak. The sub-correlator outputs, $\eta[k, a]$, can be regarded as Gaussian variables with zero mean. The timing metric is therefore the absolute value of a sum of products between zero mean Gaussian variables,

$$|\lambda[k, a]|_{a \neq 0} = \left| \sum_{l=0}^{L-1} \eta_a[k - lK, a] \eta_a^*[k - (l+P)K, a] \right| . \quad (7)$$

In Appendix A the distribution of the timing metric is analyzed for different choices of the number of differential signals. In Fig. 4 the cumulative distribution function (CDF) of the timing metric is presented for various correlator lengths, $K$, and number of differential signals, $L$, when the observation interval is 512 samples, SNR=10dB and $\rho = 0.1$.

### *C. Receiver Operation Characteristics*

Depending on how the detection threshold is set we will get a specific probability of missing the sync signal and a probability of false alarm. In Fig. 5 we plot the receiver operation characteristics (ROC) for different parameter choices. It is of course desirable to be in the lower left corner where both probabilities are low. Here, again, we see the importance of using long sub-correlator lengths. By correlating samples before differential detection we are not so sensitive to single noise samples. In conventional OFDM synchronization no correlation is performed before differential detection. The

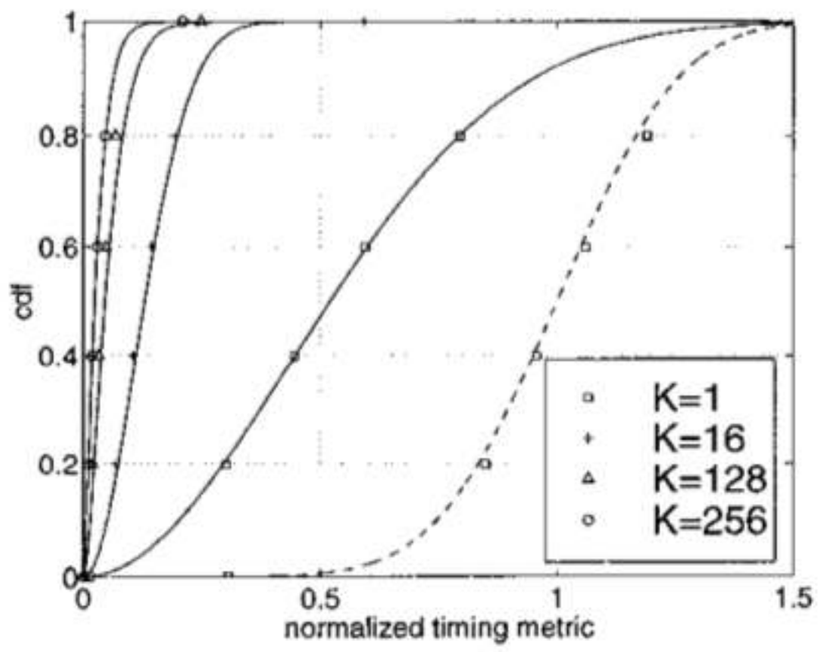


Fig. 4. CDF for the normalized timing metric when the timing is wrong (solid) and correct (dashed), SNR=10 dB, $\rho = 0.1$, observation interval 512 samples and $(K, L) = \{(1, 256), (16, 16), (128, 2), (256, 1)\}$. Marker values are obtained by simulations, whereas the lines represent theoretical values.

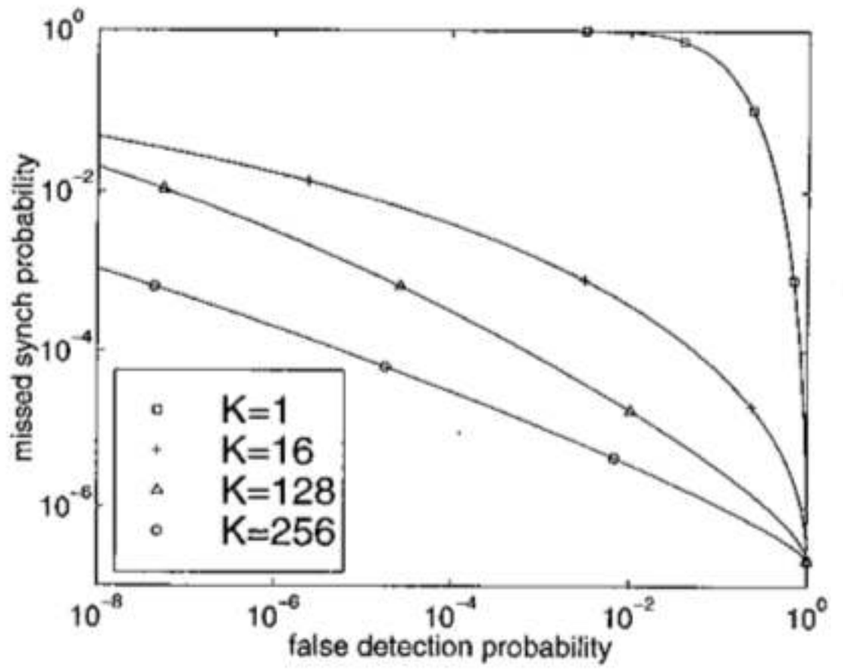


Fig. 5. Receiver operation characteristics, probability of missing the synch signal vs. false detection probability. SNR=10 dB, $\rho = 0.1$, $(K, L) = \{(1, 256), (16, 16), (128, 2), (256, 1)\}$ and observation interval 512 samples.

proposed technique will therefore give better performance, also when only used as a preamble in acquisition mode.

## V. Frequency Estimator Performance

The frequency estimator structure is the same both in tracking and acquisition mode, but a two step procedure can be used in order to enhance the performance. In acquisition mode the sub-correlator length, $K$, and the number of delay elements, $P$, are chosen according to the maximum expected frequency offset. In tracking mode, initial compensation has already been made and therefore larger $K$ and $P$ can be used to decrease the variance of the frequency estimation error.

The phase increment method used gives a (nearly) unbiased frequency estimate of a complex exponential in white noise [8] and can cope with frequency offsets which are upper bounded by $|\varepsilon_c| < M/(PK)$. The normalized frequency estimate when the timing is known is given by

$$\hat{\varepsilon}_c = \frac{M}{KP} \cdot \arg(\lambda[k, 0]) . \quad (8)$$

The frequency offset estimators in [1], [2], [4] and [5] can, from a performance point of view, be seen as a special case of the proposed estimator in acquisition mode. See Table 1 for a comparison of parameters, where $G$ denotes the length of the cyclic prefix.

The variance of the normalized frequency estimates can be calculated as [8]

$$var(\varepsilon_c) = \frac{M^2}{4\pi^2 K^3 LP} \left( \frac{1}{L} \cdot \frac{(1-\rho)\sigma_s^2 + \sigma_n^2}{\rho \sigma_s^2 \mathrm{sinc}^2(\varepsilon_c K/M)} + \frac{1}{2KP} \cdot \left( \frac{(1-\rho)\sigma_s^2 + \sigma_n^2}{\rho \sigma_s^2 \mathrm{sinc}^2(\varepsilon_c K/M)} \right)^2 \right). \quad (9)$$

TABLE 1. COMPARISON OF PARAMETERS FOR SOME FREQUENCY OFFSET ESTIMATORS BASED ON ONE SYMBOL MEASUREMENTS.

| reference | $K$ | $P$ | $L$ |
|---|---|---|---|
| van de Beek [1] | 1 | $M$ | $G$ |
| Moose [2] | 1 | $M/2$ | $M/2$ |
| Nishinaga [5] | 1 | 1 | $M-1$ |
| Fawer [4] | $M/2$ | 1 | 1 |
| PN-based | $K < \frac{M}{P\lvert\varepsilon_c\rvert}$ | $P < \frac{M}{K\lvert\varepsilon_c\rvert}$ | $\frac{M}{K} - P$ |

Strictly speaking this is only valid for zero frequency offset, but simulations indicate [8] that it is a good approximation for other frequency offsets as well. An interesting property to note is that the same minimum variance can be achieved for different sub-correlator lengths as long as the number of delay elements are chosen properly.

Fig. 6 shows theoretical and simulated values of the variance as a function of the frequency offset when the estimator is designed for a worst case normalized offset of 1, 4 and 10 respectively. Due to the flat region we can conclude that the performance is determined by the frequency offset for which the estimator is designed and that a worst case design has to be made. For large frequency offsets a two mode approach can be used to decrease the variance. First the parameters are adjusted for the worst case scenario and after a first coarse estimate has been made and corrected longer sub-correlators and larger delay can be used. As a rule of thumb the normalized frequency error must not exceed a few percent, see e.g. [2][9]. In order to fulfil this in tracking mode we need to extend the observation interval or increase the code power ratio compared to the parameters used in the figure. A possible solution could be to have correlation length 1 and an observation interval of 3 symbols. Then the frequency error variance becomes $1.3 \cdot 10^{-4}$ for small offsets in tracking mode.

## VI. CONCLUSIONS

We have presented and analyzed a new approach for synchronization in OFDM systems. The technique is very flexible and has a large frequency offset range. Offsets up to half the OFDM bandwidth can be detected in one step, instead of the common offset range equal to one or half the sub-channel spacing. The synchronization signal is achieved by correlating received samples before they are differentially detected. This makes the synchronizer less sensitive to single noise values and results in better detection properties compared to conventional synchronizers. The amount of synchronization signal is controlled by a single parameter and can be tailored to a specific application. Therefore the presented synchronizer scheme is robust and works for low signal to noise ratios. The complexity of the synchronizer is low and it is therefore suitable for implementation.

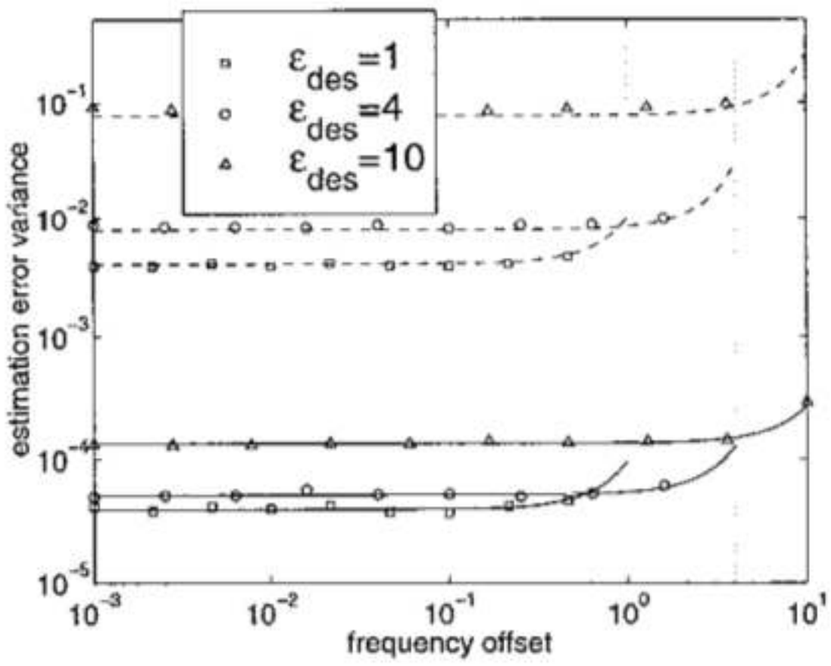


Fig. 6. Variance of the normalized frequency estimation error as a function of the offset for SNR=10 dB and code power ratio $\rho$ =0.1 (dashed) and $\rho$ =1 (solid). The sub-correlators are designed for frequency offsets 1, 4 and 10. Marker values are obtained by simulations.

## APPENDIX A. DISTRIBUTION OF THE TIMING METRIC

In this section we analyze the distribution of the timing metric when the timing is not correct. We analyze the case with one or two differential signals, $L$, or when the number of differential signals is large. The normalized complex outputs of the sub-correlators have zero mean and variance $\sigma^2_{\eta_a} = ((1-\rho)\sigma_s^2 + \sigma_n^2)/(KL\rho\sigma_s^2)$ if an ideal code with perfect autocorrelation properties is used, and variance $\sigma^2_{\eta_a} = (\sigma_s^2 + \sigma_n^2)/(KL\rho\sigma_s^2)$ for a random code.

For $L$=1 we can rewrite the timing metric as

$$|\lambda[k,a]| = |\eta_a[k-lK,a]||\eta_a[k-(l+P)K,a]|, \quad (10)$$

where the two terms are Rayleigh distributed. By the transformation theorem we can derive the joint PDF for $|\lambda[k,a]|$ and $|\eta_a[k-lK,a]|$ and then integrate over $|\eta_a[k-lK,a]|$ to get the probability density function (PDF) for the timing metric. The PDF for incorrect timing becomes

$$f_{|\lambda[k,a]|}(d) = \left(\frac{2}{\sigma^2_{\eta_a}}\right)^2 d k_0\left(2\frac{d}{\sigma^2_{\eta_a}}\right), \quad (11)$$

where $k_0(x)$ denotes the zeroth-order modified Bessel function. The CDF of the timing metric is consequently given by

$$P\{|\lambda[k,a]| \le \alpha\} = F_D(\alpha) = 1 - 2\frac{\alpha}{\sigma^2_{\eta_a}} k_1\left(2\frac{\alpha}{\sigma^2_{\eta_a}}\right), \quad (12)$$

where $k_1$ is the first order modified Bessel function.

For $L$=2 we derive bounds for the timing metric. If $L$ is even the metric can be rewritten as

$$\lambda[k,a] = \sum_{l=0}^{L-1} \eta_a[k-lK,a]\eta_a^*[k-(l+P)K,a] \quad (13)$$

$$= \sum_{k=0}^{L/2-1} d_{2k+1}c_{2k+1} + b_{2k+1}e_{2k+1}.$$

All the terms ($b$, $c$, $d$ and $e$) in (13) are independent zero mean Gaussian variables, $d$ and $b$ are real valued and have variance $\sigma_b^2 = \sigma_d^2 = E[bb] = \sigma_{\eta_a}^2/2$, whereas $c$ and $e$ are complex valued with variance of the both complex parts $\sigma_{Re\{c\}}^2 = \sigma_{Im\{c\}}^2 = \sigma_{\eta_a}^2$. Defining new variables as $g_k = d_{2k+1}Re\{c_{2k+1}\}$ and $h_k = d_{2k+1}$, the joint probability function for $g$ and $h$ becomes

$$f_{G,H}(g,h) = \frac{1}{2\pi\sigma_{Re\{c\}}\sigma_d}\exp\left(-\frac{1}{\sigma_{Re\{c\}}^2}\left(\frac{g}{h}\right)^2 - \frac{1}{\sigma_d^2}h^2\right)\frac{1}{h}. \quad (14)$$

Integrating [10, integral 3.478.4] over $h$ gives the PDF for the products, i.e.

$$f_G(g) = \int_{-\infty}^{\infty} f_{G,H}(g,h)dh = \frac{1}{\pi\sigma_{Re\{c\}}\sigma_d}k_0\left(\frac{|g|}{\sigma_{Re\{c\}}\sigma_d}\right) \quad (15)$$

$$= \frac{\sqrt{2}}{\pi\sigma_{\eta_a}^2}k_0\left(\frac{\sqrt{2}|g|}{\sigma_{\eta_a}^2}\right).$$

Naturally this PDF also applies for $b_{2k+1}e_{2k+1}$ and for the corresponding imaginary parts. The characteristic function of the product, $g$, can be calculated as [10, integral 6.671.14]

$$\Phi_g(\omega) = \int_{-\infty}^{\infty} f_G(g)e^{i\omega g}dg = \frac{\sqrt{2}}{\pi\sigma_{\eta_a}^2}\int_{-\infty}^{\infty} k_0\left(\frac{\sqrt{2}|g|}{\sigma_{\eta_a}^2}\right)e^{i\omega g}dg \quad (16)$$

$$= \frac{\sqrt{2}}{\sigma_{\eta_a}^2}\frac{1}{\sqrt{\left(\sqrt{2}/\sigma_{\eta_a}^2\right)^2 + \omega^2}}.$$

The PDF of the sum of products, i.e. the real part of $\lambda$, is given by the inverse transform of the product between the $L$ characteristic functions,

$$f_{Re\{\lambda\}}(x) = \frac{1}{2\pi}\left(\frac{\sqrt{2}}{\sigma_{\eta_a}^2}\right)^L \int_{-\infty}^{\infty}\left(\left(\frac{\sqrt{2}}{\sigma_{\eta_a}^2}\right)^2 + \omega^2\right)^{-L/2} e^{-i\omega x}d\omega. \quad (17)$$

For $L$=2, we get [10, integral 3.389.5] a Laplacian random variable with PDF

$$f_{Re\{\lambda\}}(x) = \frac{1}{\sqrt{2}\sigma_{\eta_a}^2}\exp\left(-\frac{\sqrt{2}|x|}{\sigma_{\eta_a}^2}\right). \quad (18)$$

$|Re\{\lambda[k,a]\}|$ and $|Re\{\lambda[k,a]\}|$ are therefore independent exponential variables and the sum of them is therefore an Erlang-2 distributed variable. This means that the CDF of $|\lambda[k,a]|$ is upper bounded by the CDF of an Erlang-2 variable $X_\lambda$,

$$F_{X_\lambda}(x) = 1 - \left(1 + \frac{\sqrt{2}}{\sigma_{\eta_a}^2}x\right)\exp\left(-\frac{\sqrt{2}}{\sigma_{\eta_a}^2}x\right). \quad (19)$$

The CDF of $|\lambda[k,a]|$ is lower bounded by the CDF of the maximum, $Y_\lambda$, of two independent exponential variables,

$$F_{Y_\lambda}(y) = \left(1 - \exp\left(-\frac{\sqrt{2}}{\sigma_{\eta_a}^2}y\right)\right)^2. \quad (20)$$

Finally, if $L$ is large $Re\{\lambda\}$ and $Im\{\lambda\}$ can be approximated as independent Gaussian variables due to the central limit theorem. In this case $Re\{\lambda\}$ and $Im\{\lambda\}$ have zero mean and variance

$$\sigma_{Re\{\lambda\}}^2 = \left(L(\sigma_{\eta_a}^2)^2\right)/2. \quad (21)$$

The normalized conventional timing metric is therefore Rayleigh distributed with CDF

$$P\{|\lambda[k,a]| \le \alpha\} = F_{|\lambda|}(\alpha) \approx 1 - \exp\left(-\frac{\alpha^2}{2\sigma_{Re\{\lambda\}}^2}\right). \quad (22)$$

## REFERENCES


[1] J.J. van de Beek, M. Sandell and P. O. Börjesson, "ML estimation of time and frequency offset in OFDM systems", IEEE Trans. on Signal Processing, vol. 45, no. 7, July 1997, pp. 1800-1805.

[2] P. Moose, "A technique for orthogonal frequency division multiplexing frequency offset correction", IEEE Trans. on Communications, vol.42, no. 10, Oct. 1994, pp. 2908-14.

[3] T.M. Schmidl and D. C. Cox, "Robust frequency and timing synchronization for OFDM", IEEE Trans. on Communications, vol. 45, no. 12, Dec. 1997, pp. 1616-1621.

[4] U. Fawer, "A coherent spread-spectrum diversity receiver with AFC for multipath fading channels", IEEE Trans. on Communications, vol. 42, no. 2/3/4, Feb.-April 1994, pp. 1300-1311.

[5] N. Nishinaga, M. Nakagami and Y. Iwadare, "A simple synchronization acquisition method for DS/SS system under carrier frequency offset", IEICE Trans. on Fundamentals, vol. E80-A, no. 11, Nov. 1997, pp. 2162-2171.

[6] T.P. Holden and K. Feher, "A spread spectrum based system technique for synchronization of digital mobile communication systems", IEEE Trans. on Broadcasting, vol. 36, no. 3, Sept. 1990, pp. 185-194.

[7] A. Steingass, A.J. van Wijngaarden and W.G. Teich, "Frame synchronization using superimposed sequences", in Proc. IEEE International Symposium on Information Theory, Ulm, Germany, June 29-July 4, 1997, p. 489.

[8] H. Meyr and M. Moeneclaey, Digital Communication Receivers. New York, U.S.A.: John Wiley & Sons, 1998.

[9] T. Pollet, M. Van Bladel and M. Monelcaey, "BER sensitivity of OFDM systems to carrier frequency offset and Wiener phase noise", IEEE Trans on Communications, vol. 43, no. 2/3/4, Feb.-April 1995, pp. 191-193.

[10] I.S. Gradshteyn And I.M. Ryzhik, Table Of Integrals, Series, And Products. Alan Jeffrey, Editor, London, UK: Academic Press, 1994.